Universidade de São Paulo

Biblioteca Digital da Produção Intelectual - BDPI

Departamento de Minas de Petróleo - EP/PMI | Artigos e Materiais de Revistas Científicas - EP/PMT

2015

Using bone ash as an additive in porcelain sintering

Ceramics International, Oxford, v. 41, n.1, p. 487-496, 2015
http://www.producao.usp.br/handle/BDPI/47650

Downloaded from: Biblioteca Digital da Produção Intelectual - BDPI, Universidade de São Paulo

Available online at www.sciencedirect.com

ScienceDirect

Ceramics International 41 (2015) 487–496

CERAMICS INTERNATIONAL

www.elsevier.com/locate/ceramint

Using bone ash as an additive in porcelain sintering

Douglas Gouvêa[a,*], Taisa Tisse Kaneko[a], Henrique Kahn[b], Edilene de Souza Conceição[a], Juliana L. Antoniassi[b]

[a]*Laboratório de Processos Cerâmicos, Departamento de Engenharia Metalúrgica e de Materiais Escola Politécnica da Universidade de São Paulo (EPUSP), Av. Prof Mello Moraes, 2463, Cidade Universitária, CEP 05580-900 São Paulo, SP, Brazil*

[b]*Laboratório de Caracterização Tecnológica, Departamento de Engenharia Minas e Petróleo, Escola Politécnica da Universidade de São Paulo (EPUSP), Av. Prof Mello Moraes, 2473, Cidade Universitária, CEP 05580-900 São Paulo, SP, Brazil*

Received 23 May 2013; received in revised form 11 July 2014; accepted 23 August 2014
Available online 6 September 2014

Abstract

Calcined bovine bone (CBB) is generally used to manufacture high-quality porcelain known as bone china. In these products, the amount of bone ash is about 50%. However, it is known that CBB, in small quantities added to raw materials such as feldspars, can reduce the *liquidus* temperature and thus promote liquid-phase sintering. The purpose of this study was to evaluate the potential use of bone ash as a sintering promoter of porcelain made by a classical triaxial system. Hard porcelain was prepared with 0, 1, 2, and 5 wt% CBB and sintered at temperatures ranging from 1100 to 1400 °C. For the sample containing 2% CBB, the sintering temperature was reduced by 50 °C relative to 0% CBB, while the sample's tensile strength was the highest among all samples. Two mechanisms could be observed during porcelain sintering depending on CBB quantities: for 1 and 2% of CBB, the mullite formation determined the final shrinkage without changes on initial sintering temperatures; for 5% the initial sintering temperature was decreased by liquid formation.
© 2014 Elsevier Ltd and Techna Group S.r.l. All rights reserved.

Keywords: A. Sintering; B. Porosity; C. Strength; D. Porcelain; Bone ash

1. Introduction

Porcelain has unique characteristics that distinguish it from other kinds of china, such as high mechanical strength, firing temperatures above 1350 °C, porosity below 0.3%, and high whiteness and translucency [1]. Porcelain is a ceramic material of the alumina–silica–alkali oxides (primarily K_2O) ternary system, and is produced by sintering a mixture of kaolin, feldspar, and quartz at a composition close to 50:25:25, respectively [1,2]. Plastic clays can replace part of the kaolin content to increase the mechanical strength and plasticity of green bodies. Albite or orthoclase are usually used as flux and contain high sodium or potassium oxide content, respectively [1,2]. Less common raw materials used as fluxes include phyllite, pegmatites, and, more recently, phonolites, soda-lime scrap-glass and slag [3–11]. However, different types and proportions of fluxes can modify the firing temperature and final mechanical resistance of the products. For this reason, orthoclase is generally used as a flux for porcelain [1].

The characteristic particulars of the glass phase formation process during porcelain firing restrict the use of new flux compounds in china. Because porcelain consists generally of a 70% glassy phase and a 30% crystalline phase, the viscosity of the glassy phase and the amount of the crystalline phase control the pyroplastic deformation resistance of these materials [12]. Calcite and dolomite can be used to accelerate the melting of feldspars and to reduce the firing temperature without significantly changing the pyroplastic deformation behavior. However, carbonates have, as a significant drawback, the formation of CO_2 at temperatures above 900 °C. For ceramic materials produced by a single firing or rapid thermal cycles, the formation of gases at high temperatures can cause performance-affecting defects in the end products.

Calcium phosphate can be used as an alternative to carbonates for reducing the melting temperature of feldspar

*Corresponding author. Tel.: +55 11 3091 5238.
E-mail address: dgouvea@usp.br (D. Gouvêa).

http://dx.doi.org/10.1016/j.ceramint.2014.08.096
0272-8842/© 2014 Elsevier Ltd and Techna Group S.r.l. All rights reserved.

in porcelain. Calcined bovine bone (CBB), or bone ash, use is restricted to amounts of about 50% [2] in the manufacturing of bone china, making bone china generally more durable and translucent than kaolin-based porcelain [13].

The reactions of calcined bovine bones (CBB) were extensively studied by Iqbal et al. [14,15]. Although the article deals with the microstructural evolution of phosphatic porcelain, most of the chemical reactions between the CBB, kaolin, quartz and feldspar should be similar despite the low proportion of CBB used as a sintering additive of hard porcelain. As shown previously, CBB is mainly hydroxyapatite and alone is stable until 1000 °C [15,16]. However, CBB decomposes to β-TCP and calcium oxide at temperatures higher than 775 °C probably due to the presence of metakaolin [15]. The lime originated from the hydroxyapatite decomposition was supposed to react with clay materials to give a new anorthite phase at temperatures next to 800 °C and liquid phase was detected only for $T > 900$ °C [14]. Gas bubbles were supposed to be the origin of the anomalous density decreases when sintering temperatures are higher than 1200 °C [14]. Bone china sintered at 1245 °C by 1 h has a final composition of crystalline grains of anorthite, β-tricalcium phosphate and small amounts of quartz immerse in a glassy matrix [17].

Closed porosity were observed above 1280 °C for porcelain stoneware tiles as a consequence of the increase of pressure of the gas inside the closed pores, which tends to expand the pores when glass viscosity decreases [18]. Thermal analysis of porcelain stoneware (50% kaolinitic clay, 40% feldspar and 10% quartz) showed the endothermic transformation next to 550 °C is due to both clay dehydroxylation and α→β quartz transformation and the exothermic reaction next to 1000 °C was attributed to mullite crystallization [18]. Mullite, quartz and glass were found after sintering at 1280 °C simultaneously to the decrease of the mechanical properties [18]. Therefore, the best results of strength were obtained at 1270 °C which reached 34 MPa [18].

The main thermal transformations during porcelain firing were described by Carty and Senapati [1] and can be summarized as: 550 °C—dehydroxylation of kaolinite; 573 °C—α to β-quartz inversion; 700–1000 °C—alkali feldspar transformation to sanidine and depends on the sodium: potassium ratio; 950–1000 °C metakaolin transforms to a spinel-type structure; 990 °C—amorphous silica liberated during the metakaolin decomposition; 990 °C—a eutectic melt of potash feldspar with silica (depends on the type of feldspar); next to 1200 °C melt becomes saturated with silica-quartz dissolution ends and quartz-to-cristobalite transformation begins [1]. The kinetic of mullite formation could be affected by the viscosity of liquid phase formed during metakaolin decomposition [19,20]. Marinoni et al. showed that the premature glass formation due to the substitution of some feldspar by soda-lime glass in the porcelain formulation accelerated the mullite growth reaction kinetics [21].

Despite the abundance of cattle in Brazil, CBB has rarely been exploited as a raw material in the ceramic industry, and the production of bone china is relatively unknown in Latin America. CBB is primarily hydroxyapatite, which in combination with kaolin and feldspar, could form glasses [22]. Unlike most kaolin porcelains, bone china contains amorphous and crystalline phases—approximately 30 and 70%, respectively. While the amorphous phase is rich in SiO_2 and Al_2O_3, but also contains K_2O and CaO, the crystalline phase is mainly calcium phosphate [2]. CBB could therefore be used to change the *liquidus* temperature [23–25], promote liquid phase formation, and reduce the sintering temperature via liquid phase sintering.

The purpose of this study is to verify the effect of small quantities of CBB on the sintering, microstructure, and properties of traditional kaolin-based porcelain. Porcelain containing 0, 1, 2, and 5 wt% CBB was sintered at temperatures ranging from 1000 to 1400 °C.

2. Materials and methods

Water absorption and flexural strength were measured for all samples, and the degree of the decomposition and/or phase formation was determined by X-ray diffraction using the Rietveld method. Microstructural information was obtained by scanning electron microscopy (SEM), and chemical analysis was carried out using energy dispersive X-ray spectroscopy (EDS).

A 2:1:1 base porcelain composition of kaolin, to orthoclase, to quartz, respectively, was provided by Porcelanas Teixeira Company. The raw material was initially milled in an industrial ball mill for 24 h. CBB in amounts of 1, 2, and 5 wt% was introduced to the base composition by milling in a laboratory ball mill for 24 h with porcelain grinding elements. A reference sample without CBB was milled under the same conditions. Details of the powder preparation are given elsewhere [16]. The autoclaved material was then calcined at 700 °C, and ground in a laboratory ball mill. The raw material was dispersed using a commercial sodium polyacrylate, and specimens with a standard size of $80 \times 30 \times 3$ mm were obtained by slip casting in a plaster mold.

The specimens were heated at a rate of 2 °C/min from room temperature to the sintering temperature in a muffle furnace. The maximum sintering temperatures ranged from 1100 to 1400 °C in 50 °C increments without any soaking time. Three-point bend testing of the sintered samples was performed using a Kratos® universal machine with a support span of 40 mm. Deformation was carried out at a rate of 6 mm/min until fracture. Water absorption was measured in each sample by initially determining the dry weight at 110 °C, and then determining the wet weight after immersion in boiling water for 2 h and then cooling. Sintering studies were performed in a dilatometer (BP Engenharia–RB 115) by heating at 2 °C/min to 1200 °C, without residence time, in flowing air (1 atm).

The samples characterized by X-ray diffraction (XRD) were ground in an agate mortar to eliminate any preferred orientation that may have developed during firing. The patterns were carried out in the range of 10 to 70° 2θ, with a step size of 0.03° and a counting time of 30 s per step, using a PANalytical X'Pert PRO diffractometer equipped with a X'Celerator detector operating with Cu-$K\alpha$ radiation using similar analysis

routine than Bish and Howard [26]. The identification of the crystalline phases was obtained by comparing the results with the database of the International Centre for Diffraction Data (ICDD, 2003). Quantitative determination of phase abundance was performed by Rietveld refinement using the Inorganic Crystal Structures Database (ICSD, 2007) and fluorite (CaF2) as the internal standard. The main parameters refined were background, scale factor, and unit cell size, in addition to the W profile peak factor. The quality of refinements was evaluated by, the least squares residues index (χ^2) and the difference plot. Quantitative chemical analyses were carried out by X-ray fluorescence spectrometry (XRF) on a MagixPro —PANalytical instrument. A mass ratio of 1:7 (sample: spectromelt A10—Merck) was put in a platinum crucible and heated at 1100 °C to form a homogeneous glass.

Observations using SEM were made on polished sections using a 600 FEG Quanta (FEI) with an energy dispersive spectrometer (EDS) (QUANTAX 4030, Bruker). The ceramic samples were embedded in epoxy resin (Epofix–Struers), and then ground and polished with diamond. The sections were carbon coated and imaged at an accelerating voltage of 10 kV. For each section, secondary electron (SE) imaging and back-scattered electron (BSE) imaging were used to complement the elemental mapping (Na, Al, P, K, and Ca) obtained by EDS.

3. Results and discussion

The results of chemical analysis shown in Table 1 indicate that the chemical composition of bone ashes is hydroxyapatite. However, as a natural material, it is usual to find traces of a number of other elements (Table 1). The chemical composition of porcelain raw materials matches well with kaolinite, orthoclase and quartz sand (Table 1).

The water absorption (WA) results of the sintered samples with 0, 1, 2, and 5% CBB are shown in Fig. 1. By introducing CBB, we observed a notable reduction in the sintering temperature and a decrease in firing range (i.e., the temperature range between a fully opened pore network and closed porosity). From 0 to 2% CBB, the total densification clearly increases to the final sintering temperatures (Figs. 1 and 2). However, for 5% CBB porcelain the beginning of densification was clearly at lower temperatures (Fig. 1e and Fig. 2). The liquid phase originated from the lime and clay reaction during bone china sintering was perceived for $T > 900$ °C [14]. Therefore, the supposition of lime-rich liquid phase increases with CBB and the sintering temperature proportionally

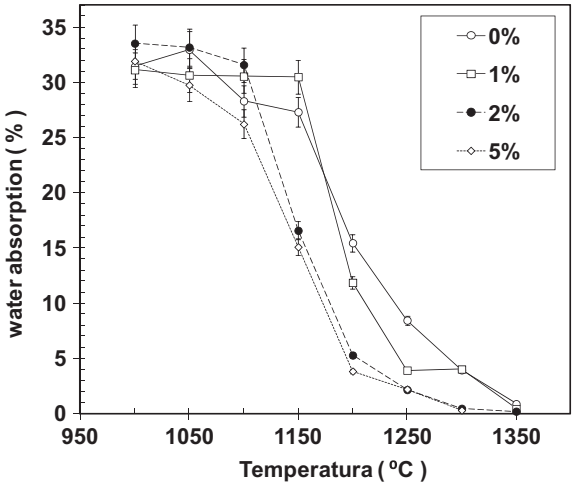

Fig. 1. Water absorption of porcelain samples containing bone ash (0, 1, 2 and 5 wt%) and sintered at different temperatures.

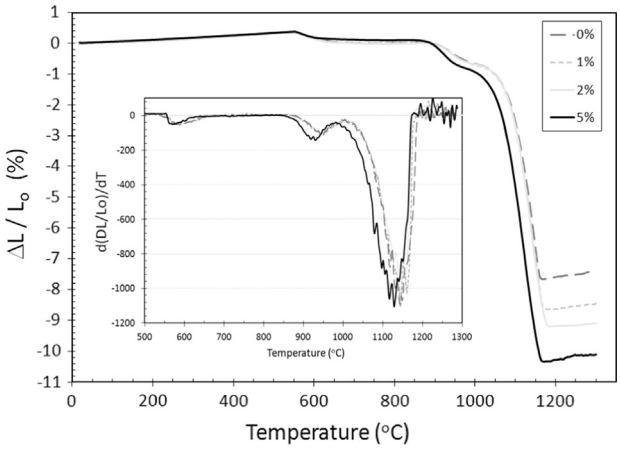

Fig. 2. Dilatometric study of porcelain containing 0, 1 and 5% of CBB in air using a heating rate of 2 °C/min.

Table 1
X-ray fluorescence spectrometry (XRF) chemical analysis of raw materials. The error estimated was less than 0.1% (LOI=loss on ignition).

	Kaolin (wt%)	Feldspar (wt%)	Quartz sand (wt%)	Bone Ash (wt%)
SiO_2	47.7	66.8	99.9	0.02
Al_2O_3	38.1	17.9	< 0.10	0.01
Fe_2O_3	0.35	0.13	< 0.10	< 0.10
MnO	< 0.10	< 0.10	< 0.10	< 0.10
MgO	0.24	0.26	< 0.10	1.11
CaO	< 0.10	0.27	< 0.10	55.3
Na_2O	< 0.10	2.30	< 0.10	1.33
K_2O	1.09	11.5	< 0.10	0.40
TiO_2	< 0.10	< 0.10	< 0.10	< 0.10
P_2O_5	0.16	< 0.10	< 0.10	41.9
LOI (1000 °C)	12.4	0.84	0.00	0.00

decreased with the glass amount originated from lime and clay reaction seems to be plausible. Nevertheless, the similar results of open porosity obtained for 2 and 5% CBB could indicate some balance between the glass amount and viscosity or mullite formation. The viscosity-temperature behavior of glasses depends on how cations replacing silica. For soda-lime glasses, the addition of CaO drastically reduces the temperature required to achieve a viscosity of $\eta = 10^3$ dPa s but only for low CaO amounts and viscosity increase for concentration high then 10% [27]. How it will be discussed

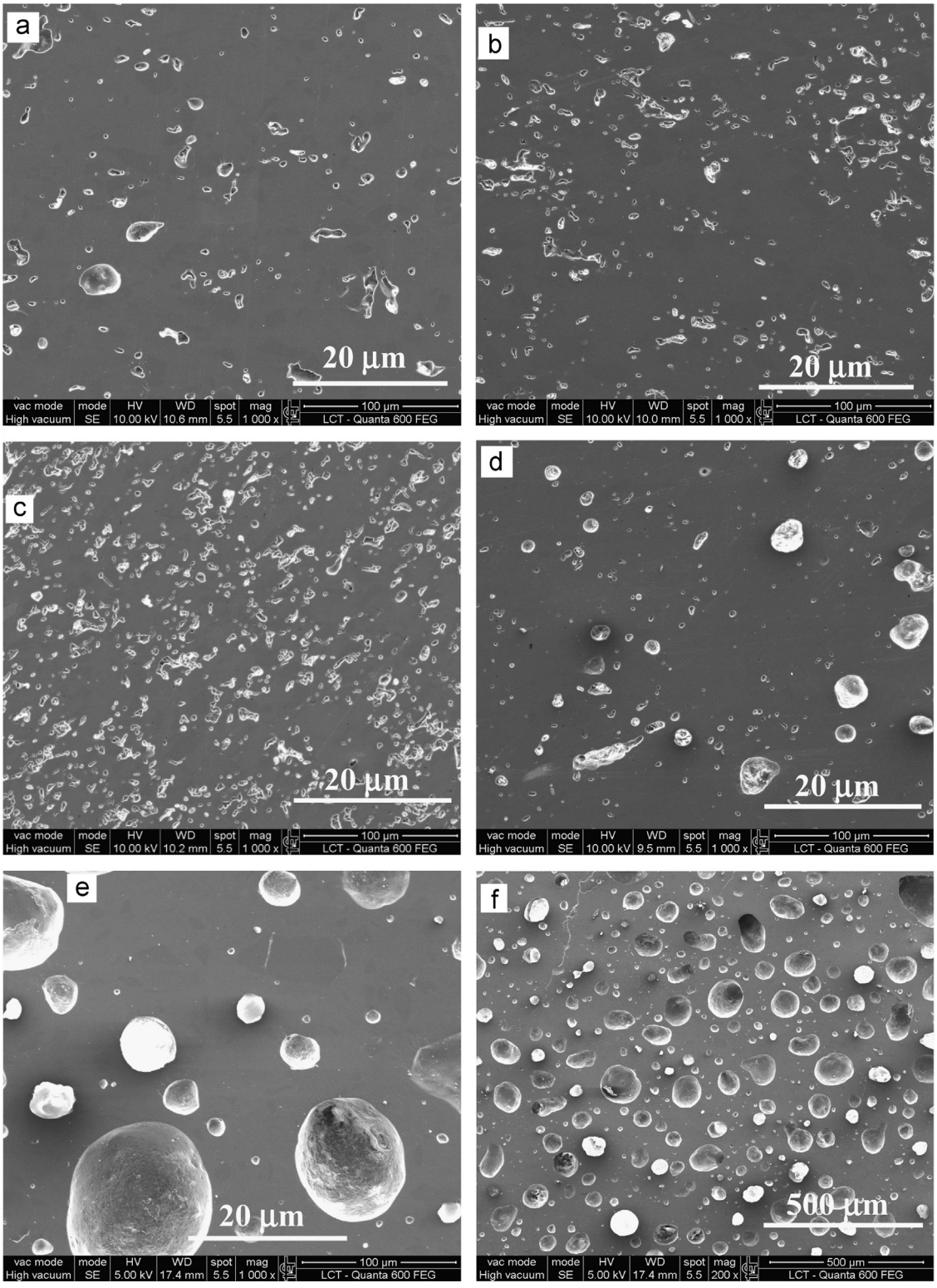

Fig. 3. SEM micrographs of porcelain samples containing different amounts of bone ash. 0% CBB 1400 °C (a); 1% CBB 1300 °C (b); 2% CBB 1250 °C (c); 5% CBB 1250 °C (d); 5% CBB 1350 °C (e) and (f).

later, the liquid phase increases the quartz dissolution during sintering and the free additional SiO_2 on the glass phase could increase the viscosity for high CBB amount.

The dilatometric study showed an interesting tendency wherein the sintering temperature decreases only for 5% CBB, but the total shrinkage increases proportionally to CCB quantities (Fig. 2). It is interesting to note that a contraction at 570 °C is observed for all samples, which is probably related to both kaolinite dehydroxylation to form metakaolin ($A1_2O_3 \cdot 2SiO_2$) and the phase transition from alpha to beta quartz transformation [1,18]. However, the contraction observed for temperatures between 850 and 1000 °C, which can be attributed to the transformation of metakaolin to a spinel-type structure and amorphous free silica because was observed for all compositions [1,17,28], is clearly shifted to lower temperatures for the sample containing 5% CBB, and could indicate a reaction between metakaolin and CBB to form a viscous liquid and promoting sintering. The formation of free silica during metakaolin decomposition could be responsible for a reduction in the temperature of glass formation, thereby further reducing the densification temperature. However, the shrinkage increases without changes on the initial sintering temperature from 0 to 2% CBB seems to involve some other mechanism then liquid formation and will be better interpreted with the phases analysis by Rietveld method.

However, SEM analysis of the polished surfaces reveals that, despite low water absorption, there is a large volume of closed porosity for some combinations of temperature and composition (Fig. 3). It is important to note that the unusual pore formation occurs after total pore elimination, and its severity increases with increasing temperature (Fig. 3d and e). This is characteristic of the dehydroxylation of hydroxyapatite ($Ca_{10}(PO_4)_6(OH)_2$) to oxyapatite ($Ca_{10}(PO_4)_6O$), which results in the release of a significant amount of water vapor [29]. Even though hydroxyapatite is known to be stable at temperatures as high as 1300 °C [30], reaction with the glass liquid phase could be responsible for the solid phase decomposition and gas elimination at lower temperatures. However, some bubbles were also observed for overfired porcelain without CBB [31,32]. The bubble formation in this case was credited to clay decomposition (dehydroxylation to form metakaolin), which occurs in less viscous regions during the early stages of overfiring. The decrease in glass viscosity caused by calcium and phosphorus solubilization could accelerate bubble formation in compounds containing CBB [14]. Fig. 4 shows that all hydroxyapatite was reacted at 1250 °C and 5% CBB and only mullite, quartz and glass phases are stables. This result indicates that all calcium and phosphorus should be soluble in the glass phase with a consequent decrease in the glass transition temperature and allowing bubbles to growth.

The rounded shape of the pores is also an indication that steam, or another gaseous phase, had formed at some stage of the firing process and nucleated inside the low viscosity amorphous phase. During isothermal sintering, the amount of rounded pores increased with the quantity of CBB, demonstrating a direct relationship between gas formation, the amount of CBB, and the sintering temperature, as shown Fig. 3a–d. When firing is carried out at 1300 °C, for the sample with 1% CBB (Fig. 3b), the residual porosity is similar to the sample without CBB (Fig. 3a). However, at a sintering temperature of 1250 °C, the addition of 5% CBB leads to the significant formation of rounded and closed pores (Fig. 3d).

Besides the amorphous phase, the crystalline phases found were mullite, formed from the decomposition of metakaolin during firing, and residual quartz (Fig. 4). These phases are

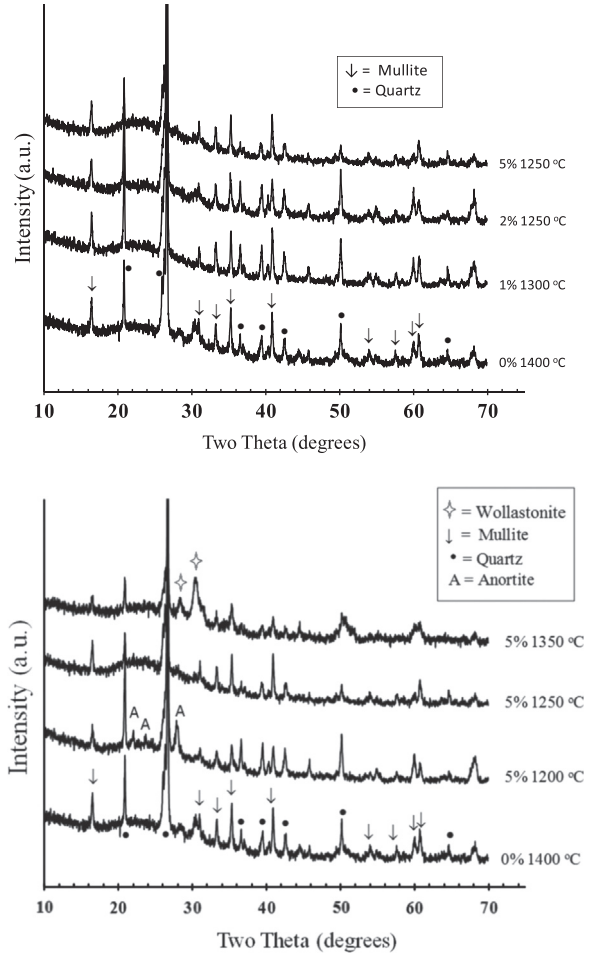

Fig. 4. XRD of porcelain samples containing different amounts of CBB and sintering in different temperatures.

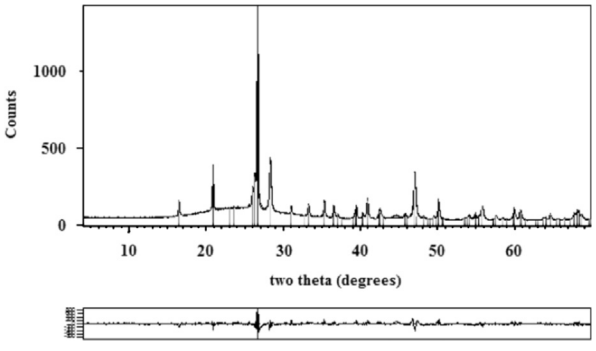

Fig. 5. Example of quantitative phase analysis by Rietveld—observed, calculated and difference X-ray powder diffraction profiles for 2% CBB—1300 °C sample.

commonly formed in porcelain sintered in the employed temperature range. The only additional crystalline phases observed arises from the reaction of the CBB with the raw materials, and were identified by XRD for samples containing 5% CBB sintered at 1200 °C—anorthite similar to common bone china [10] or 1350 °C—wollastonite [33,34]. However, anorthite is presumably consumed by the glass phase and at 1250 °C or higher, only mullite and quartz were observed.

The quantification of crystalline and glass phases was obtained by Rietveld refinement of the XRD patterns only

Table 2
Quantification of glass, mullite, quartz and orthoclase phases obtained by XRD and Rietveld refinement to different porcelain compositions and sintering temperatures.

CBB (%)	Temperature (°C)	Quartz (%)	Mullite (%)	Glass (%)
0	1400	8	14	78
0	1350	12	13	75
1	1350	15	19	66
2	1350	14	18	67
2	1300	18	17	65
5	1300	14	13	73

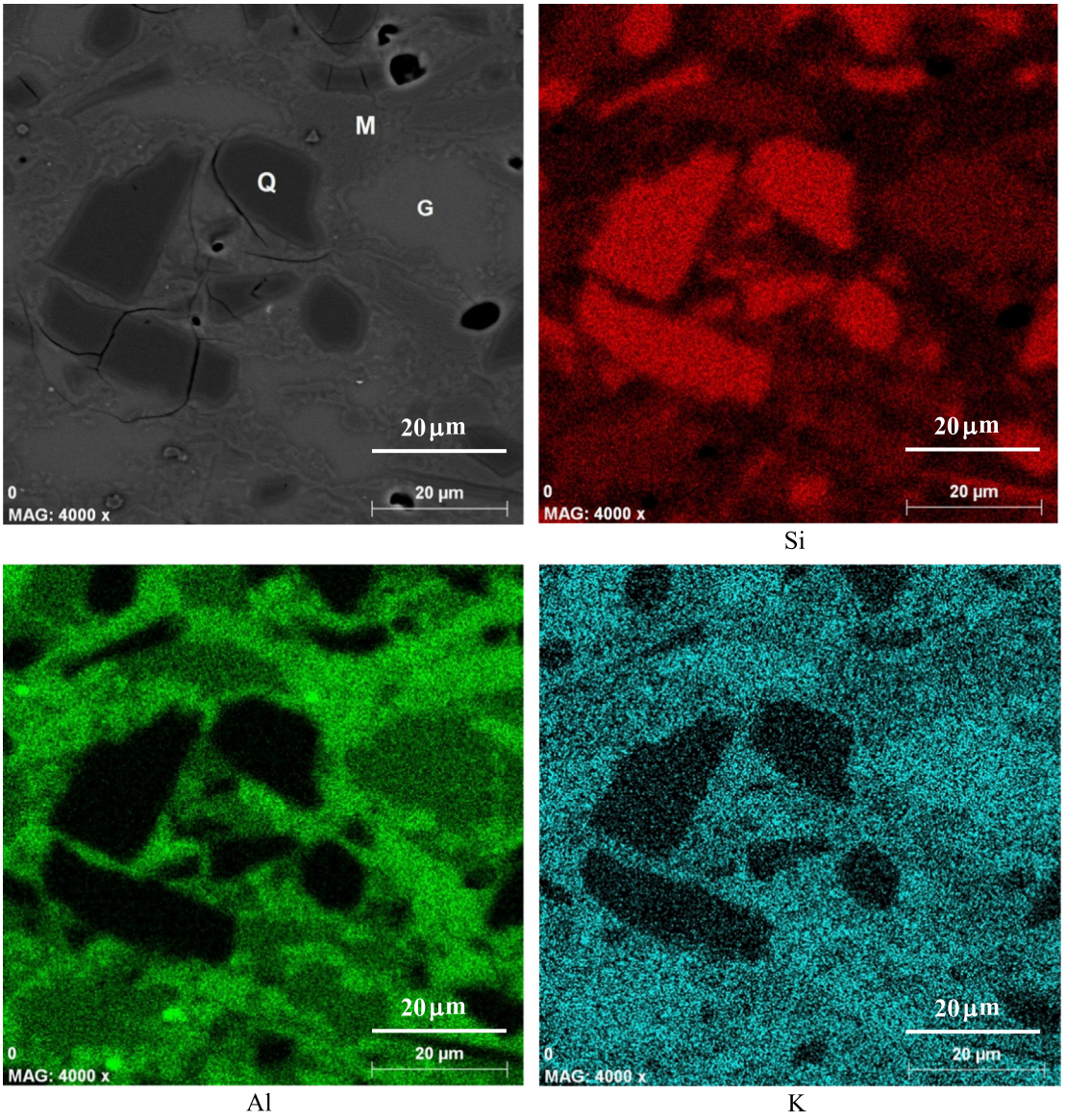

Fig. 6. SEM and chemical analysis of porcelain without CBB after sintering at 1400 °C—bar scales are the same for all images (M=mullite, G=glass and Q=quartz).

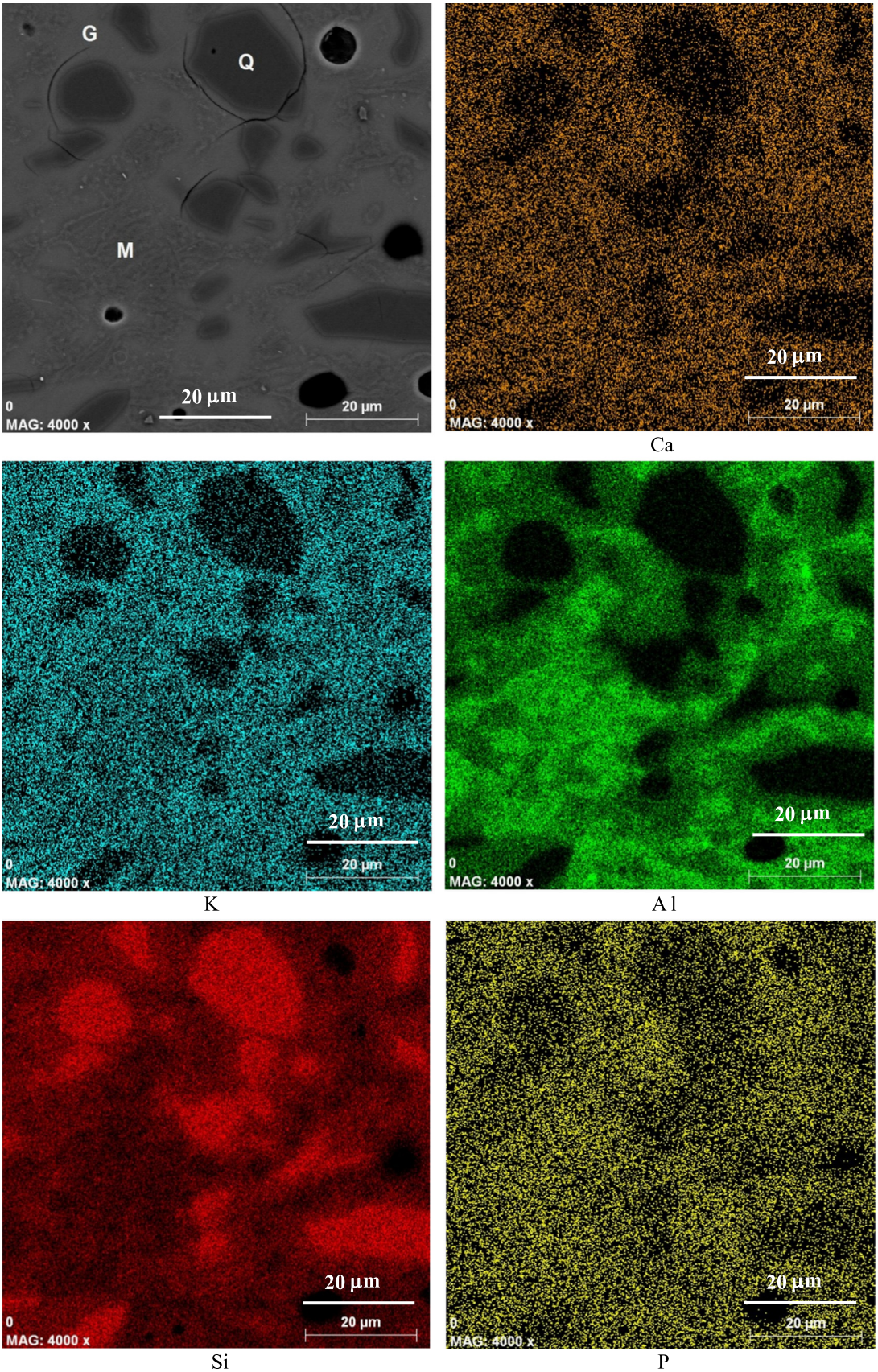

Fig. 7. SEM and EDS elemental mapping of porcelain containing 5% CBB after sintering at 1350 °C—bar scales are the same for all images. G = glass; Q = quartz and M = mulite.

for samples containing exclusively mullite and quartz as crystalline phases (Fig. 5 and Table 2) which shows good χ^2 adjustment parameters from 3 to 5 for all samples.

CBB has a high effect in mullite crystallization and the liquid phase seems to be significant only at higher concentration and temperature (Table 2). These results corroborate with dilatometric one (Fig. 2). From 0, 1 and 2% CBB, only the final shrinkage increase proportionally to the CBB but the densification starts at the same temperature. The mullite phase has a specific gravity around 3.26 g/cm^3 and then significantly higher than glass density. As the quartz amount is about the same, the increase of mullite and the proportional reduction of glass contents produce a high final density and consequently more shrinkage. However, the densification temperature for porcelain containing 5% CBB is markedly lower probably due to the increase in the glass proportion and at lower temperature. For the latter case, shrinkage can be considered mainly due to the liquid phase sintering.

The chemical analysis performed by EDS during SEM shows that most of the calcium and phosphorous is soluble in the glass phase, and that the final size of the residual quartz varies with changes in the chemical composition of the glass phase (Figs. 6–8). Islands of the glass phase surround by mullite grains could be observed in the porcelain sintered at 1400 °C (Fig. 6). The distribution of the liquid phase changes with the addition of CBB, and a more homogeneous allocation among the mullite grains could be observed for samples containing 5% CBB sintered at 1350 °C (Fig. 7). The decrease

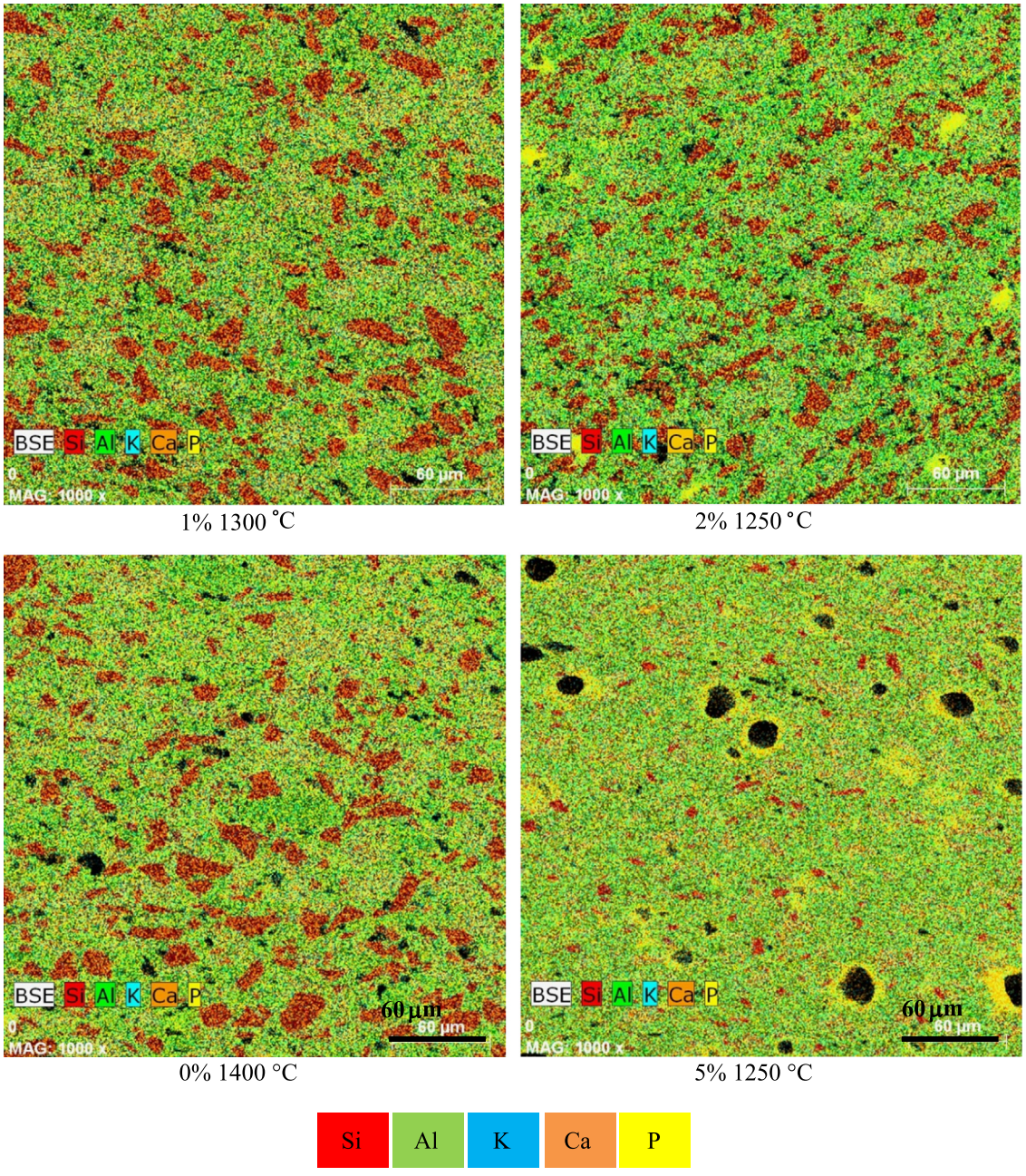

Fig. 8. SEM and EDS elemental mapping of porcelain with 0% CBB after sintering at 1400 °C, and with 2% CBB after sintered at 1300 °C.

in the final size of quartz grains observed in the Fig. 8 was also detected by a decrease in the total amount of quartz phase obtained by XRD–Rietveld refinement (Table 2). The mullite amount increases from 12% for samples containing 0% CBB sintered at 1350 °C to 18% for 2% CBB sintered at same temperature, while the amount of glass decreases from 75 to 67%. We must point out here that although the difference in glass quantities between the two samples, the presence of CBB significantly promoted the final shrinkage which has been associated to the change in the final composition of mullite and quartz (Table 2). The effect of CBB becomes clear by comparing the phases present for samples containing CBB and sintered at different temperatures (Table 2). The presence of calcium and phosphorous significantly promote mullite formation for 1 and 2% CBB increasing the shrinkage due to low glass formation and the augment of medium density due to mullite (calculated density of mullite = 3.16 g/cm^3). It is known that the glass viscosity is high during metakaolin decomposition limiting the primary mullite crystallization. Therefore, the glass viscosity decrease due to CBB dissolution could be the reason for the increase the kinetic of mullite crystallization. Mechanic properties of sintered porcelain are found to depend on the final grain size of residual quartz and the improvement on strength was supposed due to the reduction of thermal mistake between glass and quartz phases and resulting in a reduction of the failure-initiating flaw size [7]. Therefore, the final mechanical strength of porcelain containing CBB should be a balance between the defects formation due to porosity which increases with CCB quantities and the flaw size due to thermal mistake which decrease with CCB amount.

The mechanical behavior of the porcelain reflects the microstructural evolution of the ceramic bodies (Fig. 9). Increasing closed porosity was related to a decrease in flexural strength. Samples containing 2% CBB and heated to 1300 °C showed similar porosity (Fig. 1) and microstructure to that of the sample with 0% CBB sintered at 1350 °C. However, the 2% CBB samples exhibited higher mechanical resistance (Fig. 9). A reduction in porosity associated with the decrease in grain size of residual quartz could be responsible for the superior performance. These results demonstrate that the introduction of CBB reduces the firing temperature of porcelain and increases its mechanical strength, depending on the use of an appropriate sintering temperature and CBB concentration.

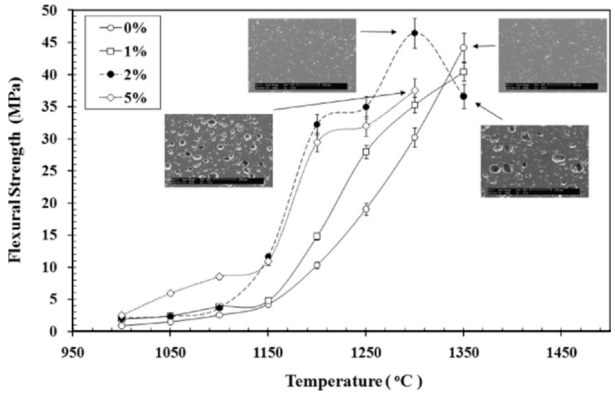

Fig. 9. Flexural Strength of porcelain samples containing 0, 1, 2 and 5 wt% of bone ash and sintering at different temperatures.

4. Conclusions

The purpose of this study was to evaluate the potential use of bone ash as a sintering promoter in porcelain made by a classical triaxial system: 50% kaolin, 25% feldspar, and 25% quartz. Hard porcelain was prepared with 0, 1, 2, and 5 wt% calcined bovine bone (CBB) and sintered from 1100 to 1400 °C. The densification increased with the CBB amount. Closed porosity was achieved at 1300 °C for samples with 2 and 5% CBB. However, microstructural analysis reveals that in samples containing 5% CBB, large pore formation was observed and can be attributed to water vapor formation during hydroxyapatite dehydroxylation, or to the decreased viscosity of the glassy phase and the acceleration of the overfiring process. The addition of CBB also accelerates mullite formation from 0 to 2% CBB promoting the total shrinkage and for 5% the liquid formation decreased the initial sintering temperature.. For most samples, only glass, mullite, orthoclase, and residual quartz were observed by XRD. Porcelains containing 2% CBB were densified at temperatures 50 °C lower than porcelain without CBB, and presented a higher modulus of rupture. However, bubble formation occurring during the overfiring of some compositions can decrease the flexural strength of the porcelain. These results indicate that, given the abundance of cattle bones in Brazil, CBB should be exploited as an alternative source of flux for the porcelain industry.

Acknowledgements

The authors would like to thank the financial support from FAPESP (Desenvolvimento do Processo Nacional para a Fabricacao de Porcelana de Ossos—Bone China—proc. 03/12721-2), FAPESP Proc. 05/55335-0, CNPq (Projeto MACEPLAS—Edital Universal 01/2002 proc. 475029/2003-8), FINEP 5089/06 and CAPES. The authors express sincere thanks to Dr Tien Tran for the English revision.

References

[1] W.M. Carty, U. Senapati, Porcelain—raw materials, processing, phase evolution, and mechanical behavior, J. Am. Ceram. Soc. 81 (1) (1998) 3–20.
[2] P. Rado, An Introduction to the Technology of Pottery, second ed., Pergamon Press, Oxford, 1988.
[3] M.G. Fonseca, G.R. Paula, R. A. Teixeira, F.G. Melchiades, A. O. Boschi, in: 43° Congresso Brasileiro de Cerâmica, 1999, pp. 44301-44311.
[4] A.M. Bernardin, D.S. de Medeiros, H.G. Riella, Pyroplasticity in porcelain tiles, Mater. Sci. Eng., A: Struct. Mater. Prop. Microstruct. Process. 427 (1-2) (2006) 316–319.
[5] G.T. Adylov, G.V. Voronov, N.A. Kulagina, E.P. Mansurova, M.K. Rumi, Properties of high-voltage porcelain with alumina-containing raw material from Uzbekistan, Glass Ceram. 64 (11-12) (2007) 437–438.

[6] A. Tucci, L. Esposito, E. Rastelli, C. Palmonari, E. Rambaldi, Use of soda-lime scrap-glass as a fluxing agent in a porcelain stoneware tile mix, J. Eur. Ceram. Soc. 24 (1) (2004) 83–92.
[7] S.R. Bragança, C.P. Bergmann, H. Hübner, Effect of quartz particle size on the strength of triaxial porcelain, J. Eur. Ceram. Soc. 26 (16) (2006) 3761–3768.
[8] F.J. Torres, J. Alarcon, Pyroxene-based glass–ceramics as glazes for floor tiles, J. Eur. Ceram. Soc. 25 (4) (2005) 349–355.
[9] S.R. Bragança, C.P. Bergmann, Traditional and glass powder porcelain: technical and microstructure analysis, J. Eur. Ceram. Soc. 24 (8) (2004) 2383–2388.
[10] E. Karamanova, G. Avdeev, A. Karamanov, Ceramics from blast furnace slag, kaolin and quartz, J. Eur. Ceram. Soc. 31 (6) (2011) 989–998.
[11] A. Salem, S.H. Jazayeri, E. Rastelli, G. Timellini, Dilatometeric study of shrinkage during sintering process for porcelain stoneware body in presence of nepheline syenite, J. Mater. Process. Technol. 209 (3) (2009) 1240–1246.
[12] E. Suvaci, N. Tamsu, The role of viscosity on microstructure development and stain resistance in porcelain stoneware tiles, J. Eur. Ceram. Soc. 30 (15) (2010) 3071–3077.
[13] S.A.F. Batista, P.F. Messer, R.J. Hand, Fracture toughness of bone china and hard porcelain, Br. Ceram. Trans 100 (6) (2001) 256–259.
[14] Y. Iqbal, P.F. Messer, W.E. Lee, Microstructural evolution in bone china, Br. Ceram. Trans 99 (5) (2000) 193–199.
[15] Y. Iqbal, P.F. Messer, W.E. Lee, Non-equilibrium microstructure of bone china, Br. Ceram. Trans 99 (3) (2000) 110–116.
[16] D. Gouvêa, G.A.V. Alatrista, S.L.M. Brito, R.H.R. Castro, H. Kahn, Surface modification of bovine bone ash prepared by milling and acid washing process, Ceram. Int. 35 (8) (2009) 3043–3049.
[17] A. Kara, R. Stevens, Characterisation of biscuit fired bone china body microstructure. Part I: XRD and SEM of crystalline phases, J. Eur. Ceram. Soc. 22 (5) (2002) 731–736.
[18] J. Martin-Marquez, J.M. Rincon, M. Romero, Effect of firing temperature on sintering of porcelain stoneware tiles, Ceram. Int. 34 (8) (2008) 1867–1873.
[19] W.E. Lee, Y. Iqbal, Influence of mixing on mullite formation in porcelain, J. Eur. Ceram. Soc. 21 (14) (2001) 2583–2586.
[20] J. Martin-Marquez, J.M. Rincon, M. Romero, Mullite development on firing in porcelain stoneware bodies, J. Eur. Ceram. Soc. 30 (7) (2010) 1599–1607.
[21] N. Marinoni, D. D'Alessio, V. Diella, A. Pavese, F. Francescon, Effects of soda-lime-silica waste glass on mullite formation kinetics and microstructures development in vitreous ceramics, J. Environ. Manage. 124 (2013) 100–107.
[22] J.J. Cooper, Bone for Bone China, Br. Ceram. Trans 94 (4) (1995) 165–168.
[23] P.D.S. Stpierre, Constitution of Bone China. 2. Reactions in Bone China Bodies, J. Am. Ceram. Soc. 38 (6) (1955) 217–222.
[24] P.D.S. Stpierre, Constitution of Bone China. 3. High-temperature phase equilibrium studies in the system tricalcium phosphate-anorthite-silica, J. Am. Ceram. Soc. 39 (4) (1956) 147–150.
[25] B.G. Varshal, V.Y. Goikhman, L.L. Mirskikh, L.K. Shitts, Y.A. Shitts, A structural interpretation of the liquid-liquid phase-separation phenomena in glasses of the R_2O–CaO–Al_2O_3–SiO_2 system assuming the formation of alkali aluminate complexes, Sov. J. Glass Phys. Chem 7 (3) (1981) 204–212212.
[26] D.L. Bish, S.A. Howard, Quantitative phase-analysis using the rietveld method, J. Appl. Crystallogr. 21 (1988) 86–91.
[27] D. Hülsenberg, A. Harnisch, A. Bismarck, Silicate glasses: a class of amorphous materials, Microstructuring of Glasses, Springer, Berlin, 2008, p. 29.
[28] C. Zanelli, M. Raimondo, G. Guarini, M. Dondi, The vitreous phase of porcelain stoneware: composition, evolution during sintering and physical properties, J. Non-Cryst. Solids 357 (16-17) (2011) 3251–3260.
[29] T.B. Tran, Electric Field-assisted Sintering of Nanocrystalline Hydroxyapatitefor Biomedical Applications, Materials Science and Engineering, University of California, Davis, 2010, p. 209 (Vol. DOCTOR OF PHILOSOPHY).
[30] A. Rapacz-Kmita, C. Paluszkiewicz, A. Slosarczyk, Z. Paszkiewicz, FTIR and XRD investigations on the thermal stability of hydroxyapatite during hot pressing and pressureless sintering processes, J. Mol. Struct. 744 (2005) 653–656.
[31] Y. Iqbal, W.E. Lee, Microstructural evolution in triaxial porcelain, J. Am. Ceram. Soc. 83 (12) (2000) 3121–3127.
[32] Y. Iqbal, W.E. Lee, Fired porcelain microstructures revisited, J. Am. Ceram. Soc. 82 (12) (1999) 3584–3590.
[33] R.P. Sreekanth Chakradhar, B.M. Nagabhushana, G.T. Chandrappa, K. P. Ramesh, J.L. Rao, Solution combustion derived nanocrystalline macroporous wollastonite ceramics, Mater. Chem. Phys. 95 (1) (2006) 169–175.
[34] W. Joswig, E.F. Paulus, B. Winkler, V. Milman, The crystal structure of $CaSiO_3$-walstromite, a special isomorph of wollastonite-II, Z. Kristallogr. 218 (12) (2003) 811–818.